Bifunctional Luminescent Rhenium(I) Complexes Containing an Extended Planar Diimine Ligand and a Biotin Moiety

Kenneth Kam-Wing Lo* and Keith Hing-Kit Tsang

Department of Biology and Chemistry, City University of Hong Kong, Tat Chee Avenue, Kowloon, Hong Kong, People's Republic of China

Received January 26, 2004

We report the synthesis, characterization, and photophysical and electrochemical properties of four bifunctional luminescent rhenium(I) complexes that contain an extended planar diimine ligand and a biotin moiety, $[Re(N\text{-}N)(CO)_3(L)](PF_6)$ (N-N = dipyrido[3,2-*a*:2′,3′-*c*]-phenazine, dppz; L = 4-((biotinamido)methyl)pyridine (py-CH_2NH-biotin; **1**), 4-(*N*-((6-biotinamido)hexanoyl)aminomethyl)pyridine, (py-$CH_2NHCOC_5H_{10}$NH-biotin; **2**); N-N = benzo[*i*]dipyrido[3,2-*a*:2′,3′-*c*]phenazine, dppn; L = py-CH_2NH-biotin (**3**), py-$CH_2NHCOC_5H_{10}$NH-biotin (**4**)). Upon irradiation, complexes **1**−**4** exhibit intense and long-lived emission in deoxygenated fluid solutions at 298 K and in low-temperature glass. The luminescence is assigned to a triplet intraligand (^{3}IL) ($\pi \rightarrow \pi^*$) (diimine) excited state. However, the excited state of the dppn complexes **3** and **4** is likely to possess substantial triplet metal-to-ligand charge-transfer (^{3}MLCT) ($d\pi(Re) \rightarrow \pi^*$(dppn)) character. The interactions of these complexes with double-stranded calf thymus DNA have been studied by absorption and emission titrations. The binding of the complexes to avidin has also been investigated by HABA assays and emission titrations.

Introduction

Studies of the binding of small molecules to nucleic acid are very important in the development of new DNA molecular probes, diagnostic reagents, and therapeutic drugs.[1] Many transition-metal complexes have been employed as probes and cleavage reagents for nucleic acid, owing to their characteristic structural, photophysical, photochemical, and electrochemical properties. In particular, transition-metal complexes containing the extended planar ligand dipyrido[3,2-*a*:2′,3′-*c*]phenazine (dppz) and its derivatives have received much attention.[2−9] Barton and co-workers employed ruthenium(II) dppz complexes to probe the structures of double-stranded DNA and to study photoinduced electron transfer in the DNA molecules.[2a−d] The synthesis and DNA-binding properties of a number of dppz complexes of other transition-metal centers, including osmium(II),[2e] chromium(III),[4] nickel(II),[5] cobalt(III),[5] rhodium(III),[6] iridium(III),[6] and rhenium(I),[7−9] have also been reported.

In the studies of the binding of small molecules to large biomolecules, the biotin−avidin system represents a classic ligand−protein example, owing to the high binding affinity (first dissociation constant, K_d = ca. 10^{-15} M).[10−12] In view of this very strong and specific binding interaction, and the usual retention of the biological activity of biomolecules after biotinylation, the biotin−avidin technology has been extensively exploited in many bioanalytical applications.[10−12] Under most circumstances, avidin conjugated with a reporter label is used to recognize biotinylated biomolecules such as oligonucleotides, peptides, and proteins. Since avidin

* To whom correspondence should be addressed. Tel: (852) 2788 7231. Fax: (852) 2788 7406. E-mail: bhkenlo@cityu.edu.hk.

(1) See, for example: (a) Lippard, S. J. *Acc. Chem. Res.* **1978**, *11*, 211. (b) Tullis, T. D., Ed.; *Metal-DNA Chemistry*; ACS Symposium Series 402; American Chemical Society: Washington, DC, 1989. (c) Sigman, D. S.; Mazumdr, A.; Perrin, D. M. *Chem. Rev.* **1993**, *93*, 2295. (d) Nordén, B.; Lincoln, P.; Åkerman, B.; Tuite, E. In *Metal Ions in Biological Systems*; Sigel, A., Sigel, H., Eds.; Marcel Dekker: New York, 1996; Vol. 33, p 177. (e) Erkkila, K. E.; Odom, D. T.; Barton, J. K. *Chem. Rev.* **1999**, *99*, 2777. (f) Metcalfe, C.; Thomas, J. A. *Chem. Soc. Rev.* **2003**, *32*, 215.

(2) (a) Hartshorn, R. M.; Barton, J. K. *J. Am. Chem. Soc.* **1992**, *114*, 5919. (b) Jenkins, Y.; Barton, J. K. *J. Am. Chem. Soc.* **1992**, *114*, 8736. (c) Murphy, C. J.; Arkin, M. R.; Jenkins, Y.; Ghatlia, N. D.; Bossmann, S. H.; Turro, N. J.; Barton, J. K. *Science* **1993**, *262*, 1025. (d) Arkin, M. R.; Stemp, E. D. A.; Holmlin, R. E.; Barton, J. K.; Hörmann, A.; Olson, E. J. C.; Barbara, P. F. *Science* **1996**, *273*, 475. (e) Holmlin, R. E.; Yao, J. A.; Barton, J. K. *Inorg. Chem.* **1999**, *38*, 174.

(3) (a) Hiort, C.; Lincoln, P.; Nordén, B. *J. Am. Chem. Soc.* **1993**, *115*, 3448. (b) Haq, I.; Lincoln, P.; Suh, D.; Nordén, B.; Chowdhry, B. Z.; Chaires, J. B. *J. Am. Chem. Soc.* **1995**, *117*, 4788. (c) Lincoln, P.; Broo, A.; Nordén, B. *J. Am. Chem. Soc.* **1996**, *118*, 2644. (d) Coates, C. G.; Olofsson, J.; Coletti, M.; McGarvey, J. J.; Önfelt, B.; Lincoln, P.; Nordén, B.; Tuite, E.; Matousek, P.; Parker, A. W. *J. Phys. Chem. B* **2001**, *105*, 12653. (e) Yun, B. H.; Kim, J. O.; Lee, B. W.; Lincoln, P.; Nordén, B.; Kim, J.-M.; Kim, S. K. *J. Phys. Chem. B* **2003**, *107*, 9858.

(4) Barker, K. D.; Benoti, B. R.; Bordelon, J. A.; Davis, R. J.; Delmas, A. S.; Mytykh, O. V.; Petty, J. T.; Wheeler, J. F.; Kane-Maguire, N. A. P. *Inorg. Chim. Acta* **2001**, *322*, 74.

(5) Arounaguiri, S.; Maiya, B. G. *Inorg. Chem.* **1996**, *35*, 4267.

(6) Herebian, D.; Sheldrick, W. S. *J. Chem. Soc., Dalton Trans.* **2002**, 966.

(7) Stoeffler, H. D.; Thornton, N. B.; Temkin, S. L.; Schanze, K. S. *J. Am. Chem. Soc.* **1995**, *117*, 7119.

(8) Metcalfe, C.; Webb. M.; Thomas, J. A. *Chem. Commun.* **2002**, 2026.

(9) (a) Yam, V. W. W.; Lo, K. K. W.; Cheung, K. K.; Kong, R. Y. C. *Chem. Commun.* **1995**, 1191. (b) Yam, V. W. W.; Lo, K. K. W.; Cheung, K. K.; Kong, R. Y. C. *J. Chem. Soc., Dalton Trans.* **1997**, 2067.

(10) Wilchek, M.; Bayer, E. A. *Anal. Biochem.* **1988**, *171*, 1.

(11) Wilchek, M. *Methods in Enzymology*; Academic Press: San Diego, CA, 1990; Vol. 184.

(12) Hermanson, G. T. *Bioconjugate Techniques*; Academic Press: San Diego, CA, 1996.

10.1021/om049936x CCC: $27.50
Publication on Web 05/13/2004

Chart 1. Structures of Complexes 1−4[a]

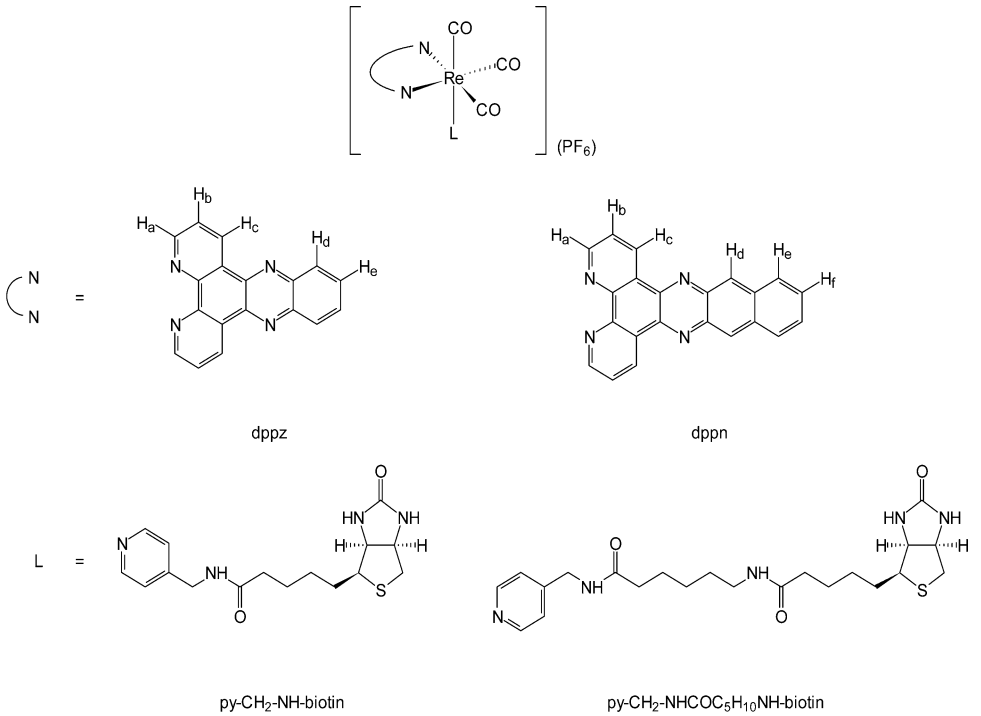

[a] Legend: **1**, [Re(dppz)(CO)$_3$(py-CH$_2$-NH-biotin)](PF$_6$); **2**, [Re(dppz)(CO)$_3$(py-CH$_2$-NHCOC$_5$H$_{10}$NH-biotin)](PF$_6$); **3**, [Re(dppn)(CO)$_3$(py-CH$_2$-NH-biotin)](PF$_6$); **4**, [Re(dppn)(CO)$_3$(py-CH$_2$-NHCOC$_5$H$_{10}$NH-biotin)](PF$_6$).

contains four biotin-binding sites, it appears that this protein can be used as a bridge and the biotinylated species can be detected by biotin−fluorophore conjugates. However, biotin−fluorophore conjugates suffer from severe fluorescence quenching when they bind to avidin, unless there are exceptionally long spacers between the biotin and the fluorophore units to reduce dye−dye interaction.[13] Recently, we reported a series of luminescent rhenium(I) polypyridine biotin complexes that can be considered as a new class of probes for avidin.[14] Unlike common fluorescent biotin compounds, the emission of the rhenium biotin complexes is enhanced when they bind to avidin.

We believe that bifunctional molecules which can interact and respond to both nucleic acid and proteins could contribute to the development of new biorecognition reagents. Here we report the synthesis and characterization of four luminescent rhenium(I) complexes that contain an extended planar diimine ligand and a biotin moiety, [Re(N-N)(CO)$_3$(L)](PF$_6$) (N-N = dipyrido[3,2-*a*:2′,3′-*c*]phenazine (dppz), L = 4-((biotinamido)methyl)pyridine (py-CH$_2$NH-biotin; **1**), 4-(*N*-((6-biotinamido)hexanoyl)aminomethyl)pyridine (py-CH$_2$NHCOC$_5$H$_{10}$-NH-biotin; **2**); N-N = benzo[*i*]dipyrido[3,2-*a*:2′,3′-*c*]phenazine (dppn), L = py-CH$_2$NH-biotin (**3**), py-CH$_2$-NHCOC$_5$H$_{10}$NH-biotin (**4**)) (Chart 1). These complexes are different from our recently reported luminescent rhenium(I) biotin complexes in that the extended planar dppz and dppn ligands are expected to enable complexes **1**−**4** to exhibit interesting intercalative interactions with double-helical DNA molecules.[9,14] At the same time, we also anticipate that the biotin groups of the complexes enable them to bind to avidin. In this report, the photophysical, electrochemical, and biomolecule-binding properties of these new complexes are described.

Experimental Section

Materials and Reagents. All solvents were of analytical reagent grade. Re(CO)$_5$Cl (Aldrich), 2,3-diaminonaphthalene (Acros), 6-aminocaproic acid (Acros), *N*-hydroxysuccinimide (Acros), *N*,*N*′-dicyclohexylcarbodiimide (Acros), KPF$_6$ (Acros), biotin (Acros), and 4′-hydroxyazobenzene-2-carboxylic acid (HABA; Sigma) were used without purification. 4-(Aminomethyl)pyridine and 1,2-diaminobenzene were purchased from Acros and were purified by distillation under nitrogen and sublimation under vacuum, respectively. Double-stranded calf thymus DNA was obtained from Calbiochem and purified by phenol extraction.[15] The DNA concentration per nucleotide was determined by absorption spectroscopy using the molar absorptivity 6600 dm^3 mol^{-1} cm^{-1} at 260 nm.[16] Unless specified otherwise, all spectroscopic titrations were carried out in 20 mM tris(hydroxymethyl)methylamine (Tris-Cl) at pH 7.2/methanol (7/3 v/v). Autoclaved Milli-Q water was used for the preparation of the aqueous solutions.

4-(*N*-((6-Biotinamido)hexanoyl)aminomethyl)pyridine, py-CH$_2$NHCOC$_5$H$_{10}$NH-biotin. 4-(Aminomethyl)pyridine (60 mg, 0.56 mmol) in 2 mL of DMF was added to a mixture of (6-biotinamido)hexanoyl-*N*-hydroxysuccinimide ester[11] (256 mg, 0.56 mmol) and triethylamine (314 μL, 2.24 mmol) in 5 mL of DMF. The solution was stirred under nitrogen at room temperature, and a yellow solid appeared after several hours. The stirring was continued for 12 h. The suspension was then evaporated to dryness to give a pale

(13) (a) Gruber, H. J.; Marek, M.; Schindler, H.; Kaiser, K. *Bioconjugate Chem.* **1997**, *8*, 552. (b) Marek, M.; Kaiser, K.; Gruber, H. J. *Bioconjugate Chem.* **1997**, *8*, 560. (c) Gruber, H. J.; Hahn, C. D.; Kada, G.; Riener, C. K.; Harms, G. S.; Ahrer, W.; Dax, T. G.; Knaus, H.-G. *Bioconjugate Chem.* **2000**, *11*, 696.

(14) Lo, K. K. W.; Hui, W. K.; Ng, D. C. M. *J. Am. Chem. Soc.* **2002**, *124*, 9344.

(15) Maniatis, T.; Fritsch, E. F.; Sambrook, J. *Molecular Cloning: A Laboratory Manual*; Cold Spring Harbor Laboratory: New York, 1982; p 458.

(16) Kumar, C. V.; Asuncion, E. H. *J. Am. Chem. Soc.* **1993**, *115*, 8547.

yellow solid. Recrystallization of the solid from methanol/diethyl ether afforded py-$CH_2NHCOC_5H_{10}$NH-biotin as white crystals in 181 mg yield (74%). ^{1}H NMR (300 MHz, DMSO-d_6, 298 K, TMS): δ 8.49 (d, 2H, J = 5.9 Hz; H2 and H6 of pyridine), 8.42 (t, 1H, J = 6.2 Hz; py-CH_2NH), 7.77 (t, 1H, J = 5.9 Hz; N*H*-biotin), 7.22 (d, 2H, J = 5.9 Hz; H3 and H5 of pyridine), 6.45 (s, 1H; NH of biotin), 6.38 (s, 1H; NH of biotin), 4.33−4.27 (m, 3H; NCH of biotin and py-CH_2NH), 4.14−4.10 (m, 1H; NCH of biotin), 3.15−3.06 (m, 1H; SCH of biotin), 3.02−2.98 (m, 2H; CH_2NH-biotin), 2.82 (dd, 1H, J_{gem} = 12.6 Hz, J_{vic} = 5.2 Hz; SCH of biotin), 2.61 (d, 1H, J_{gem} = 12.9 Hz; SCH of biotin), 2.18−2.04 (m, 4H; $CH_2C_4H_8NHCOCH_2C_3H_6$), 1.57−1.24 (m, 12H; py-$CH_2NHCOCH_2C_3H_6CH_2NHCOCH_2C_3H_6$). IR (KBr): ν(cm^{-1}) 3283 (s, NH), 3067 (m, NH), 2853 (m, C═H), 1701 (s, C═O), 1639 (s, C═O), 1547 (s, CONH). Positive-ion ESI-MS: m/z 448 [py-$CH_2NHCOC_5H_{10}$NH-biotin + H$^+$]$^+$.

[Re(dppz)(CO)$_3$(py-CH$_2$NH-biotin)](PF$_6$) (1). A mixture of [Re(dppz)(CO)$_3$(CH$_3$CN)](CF$_3$SO$_3$)[17] (218 mg, 0.29 mmol) and py-CH_2NH-biotin[14] (98 mg, 0.29 mmol) in 40 mL of THF/methanol (3/1 v/v) was refluxed under nitrogen overnight. The mixture was then evaporated to dryness to give a yellow solid. The complex was converted to the PF_6^- salt by metathesis with KPF_6 and then purified by column chromatography on alumina. The desired product was eluted with acetonitrile/methanol (10/1 v/v). Recrystallization of the crude product from acetonitrile/diethyl ether afforded complex **1** as yellow crystals in 142 mg yield (47%). ^{1}H NMR (300 MHz, DMSO-d_6, 298 K, TMS): δ 9.87 (d, 2H, J = 8.7 Hz; H$_c$ of dppz), 9.76 (d, 2H, J = 5.0 Hz; H$_a$ of dppz), 8.50−8.32 (m, 7H; H$_b$ and H$_d$ of dppz, H2 and H6 of pyridine and py-CH_2N*H*-biotin), 8.19−8.16 (m, 2H; H$_e$ of dppz), 7.16 (d, 2H, J = 6.5 Hz; H3 and H5 of pyridine), 6.40−6.35 (m, 2H; NH of biotin), 4.36−4.26 (m, 1H; NCH of biotin), 4.11−4.06 (m, 3H; NCH of biotin and py-CH_2NH-biotin), 3.08−3.00 (m, 1H; SCH of biotin), 2.78 (dd, 1H, J_{gem} = 12.6 Hz, J_{vic} = 5.8 Hz; SCH of biotin), 2.60 (d, 1H, J_{gem} = 12.3 Hz; SCH of biotin), 2.04 (t, 2H, J = 7.5 Hz; py-$CH_2NHCOCH_2$), 1.49−1.41 (m, 6H; py-$CH_2NHCOCH_2C_3H_6$). Anal. Calcd for [Re(dppz)(CO)$_3$(py-CH$_2$NH-biotin)](PF$_6$)·3H$_2$O: C, 40.92; H, 3.53; N, 10.32. Found: C, 40.69; H, 3.39; N, 10.59. IR (KBr): ν(cm^{-1}) 3447 (m, NH), 3268 (br, NH), 2034 (s, C≡O), 1921 (s, C≡O), 1701 (m, CONH), 835 (s, PF_6^-). Positive-ion ESI-MS: m/z 887 [Re(dppz)(CO)$_3$(py-CH$_2$NH-biotin)]$^+$, 553 [Re(dppz)(CO)$_3$]$^+$.

[Re(dppz)(CO)$_3$(py-CH$_2$NHCOC$_5$H$_{10}$NH-biotin)](PF$_6$) (2). The preparation of complex **2** was similar to that of complex **1**, except that py-$CH_2NHCOC_5H_{10}$NH-biotin (132 mg, 0.29 mmol) was used instead of py-CH_2NH-biotin. Recrystallization of the complex from acetonitrile/diethyl ether afforded complex **2** as yellow crystals in 155 mg yield (46%). ^{1}H NMR (300 MHz, DMSO-d_6, 298 K, TMS): δ 9.88 (d, 2H, J = 8.2 Hz; H$_c$ of dppz), 9.79 (d, 2H, J = 5.3 Hz; H$_a$ of dppz), 8.52−8.31 (m, 7H; H$_b$ and H$_d$ of dppz, H2 and H6 of pyridine and py-CH_2N*H*), 8.21−8.18 (m, 2H; H$_e$ of dppz), 7.71 (t, 1H, J = 5.0 Hz; N*H*-biotin), 7.18 (d, 2H, J = 6.5 Hz; H3 and H5 of pyridine), 6.43 (s, 1H; NH of biotin), 6.38 (s, 1H; NH of biotin), 4.31−4.27 (m, 1H; NCH of biotin), 4.15−4.08 (m, 3H; NCH of biotin and py-CH_2-NH), 3.16−3.06 (m, 1H; SCH of biotin), 2.96−2.89 (m, 2H; CH_2-NH-biotin), 2.79 (dd, 1H, J_{gem} = 12.6 Hz, J_{vic} = 5.0 Hz; SCH of biotin), 2.60 (d, 1H, J_{gem} = 13.7 Hz; SCH of biotin), 2.09−1.97 (m, 4H; $CH_2C_4H_8NHCOCH_2C_3H_6$), 1.76−1.07 (m, 12H; py-$CH_2NHCOCH_2C_3H_6CH_2NHCOCH_2C_3H_6$). Anal. Calcd for [Re(dppz)(CO)$_3$(py-CH$_2$NHCOC$_5$H$_{10}$NH-biotin)](PF$_6$)·2H$_2$O·CH$_3$CN: C, 44.22; H, 4.12; N, 11.46. Found: C, 43.93; H, 4.03; N, 11.64. IR (KBr): ν(cm^{-1}) 3437 (m, NH), 2023 (s, C≡O), 1911 (s, C≡O), 1644 (s, C═O), 840 (s, PF_6^-). Positive-ion ESI-MS: m/z 1000 [Re(dppz)(CO)$_3$(py-CH$_2$NHCOC$_5$H$_{10}$NH-biotin)]$^+$, 553 [Re(dppz)(CO)$_3$]$^+$.

[Re(dppn)(CO)$_3$(py-CH$_2$NH-biotin)](PF$_6$) (3). The preparation of complex **3** was similar to that of complex **1**, except that [Re(dppn)(CO)$_3$(CH$_3$CN)](CF$_3$SO$_3$) (233 mg, 0.29 mmol) was used instead of [Re(dppz)(CO)$_3$(CH$_3$CN)](CF$_3$SO$_3$). Recrystallization of the complex from dichloromethane/diethyl ether afforded complex **3** as orange-red crystals in 153 mg yield (45%). ^{1}H NMR (300 MHz, DMSO-d_6, 298 K, TMS): δ 9.87 (d, 2H, J = 8.2 Hz; H$_c$ of dppn), 9.75 (d, 2H, J = 5.0 Hz; H$_a$ of dppn), 9.23 (s, 2H; H$_d$ of dppn), 8.47−8.35 (m, 7H; H$_b$ and H$_e$ of dppn, H2 and H6 of pyridine and py-CH_2N*H*-biotin), 7.81−7.78 (m, 2H; H$_f$ of dppn), 7.20 (d, 2H, J = 6.7 Hz; H3 and H5 of pyridine), 6.44−6.36 (m, 2H; NH of biotin), 4.30−4.28 (m, 1H; NCH of biotin), 4.16−4.09 (m, 3H; NCH of biotin and py-CH_2NH-biotin), 3.18−3.04 (m, 1H; SCH of biotin), 2.79 (dd, 1H, J_{gem} = 12.6 Hz, J_{vic} = 5.0 Hz; SCH of biotin), 2.58 (d, 1H, J_{gem} = 12.6 Hz; SCH of biotin), 2.06 (t, 2H, J = 7.6 Hz; py-$CH_2NHCOCH_2$), 1.50−1.11 (m, 6H; py-$CH_2NHCOCH_2C_3H_6$). Anal. Calcd for [Re(dppn)(CO)$_3$(py-CH$_2$NH-biotin)](PF$_6$)·2H$_2$O·$^1/_2$CH$_2$Cl$_2$: C, 42.95; H, 3.39; N, 9.66. Found: C, 42.98; H, 3.29; N, 9.68. IR (KBr): ν(cm^{-1}) 3431 (m, NH), 3221 (br, NH), 2028 (s, C≡O), 1921 (s, C≡O), 1695 (m, CONH), 840 (s, PF_6^-). Positive-ion ESI-MS: m/z 937 [Re(dppn)(CO)$_3$(py-CH$_2$NH-biotin)]$^+$, 603 [Re(dppn)(CO)$_3$]$^+$.

[Re(dppn)(CO)$_3$(py-CH$_2$NHCOC$_5$H$_{10}$NH-biotin)](PF$_6$) (4). The preparation of complex **4** was similar to that of complex **2**, except that [Re(dppn)(CO)$_3$(CH$_3$CN)](CF$_3$SO$_3$) (233 mg, 0.29 mmol) was used instead of [Re(dppz)(CO)$_3$(CH$_3$CN)](CF$_3$SO$_3$). Recrystallization of the complex from dichloromethane/diethyl ether afforded complex **4** as orange-red crystals in 126 mg yield (36%). ^{1}H NMR (300 MHz, DMSO-d_6, 298 K, TMS): δ 9.87 (d, 2H, J = 8.2 Hz; H$_c$ of dppn), 9.75 (d, 2H, J = 4.4 Hz; H$_a$ of dppn), 9.23 (s, 2H; H$_d$ of dppn), 8.49−8.35 (m, 7H; H$_b$ and H$_e$ of dppn, H2 and H6 of pyridine and py-CH_2N*H*), 7.81−7.78 (m, 2H; H$_f$ of dppn), 7.71 (t, 1H, J = 5.6 Hz; N*H*-biotin), 7.19 (d, 2H, J = 6.5 Hz; H3 and H5 of pyridine), 6.42 (s, 1H; NH of biotin), 6.38 (s, 1H; NH of biotin), 4.28−4.26 (m, 1H; NCH of biotin), 4.16−4.10 (m, 3H; NCH of biotin and py-CH_2NH), 3.18−3.05 (m, 1H; SCH of biotin), 2.94−2.88 (m, 2H; CH_2NH-biotin), 2.79 (dd, 1H, J_{gem} = 12.3 Hz, J_{vic} = 5.3 Hz; SCH of biotin), 2.55 (d, 1H, J_{gem} = 13.0 Hz; SCH of biotin), 2.09−1.95 (m, 4H; $CH_2C_4H_8NHCOCH_2C_3H_6$), 1.78−1.07 (m, 12H; py-$CH_2NHCOCH_2C_3H_6CH_2NHCOCH_2C_3H_6$). Anal. Calcd for [Re(dppn)(CO)$_3$(py-CH$_2$NHCOC$_5$H$_{10}$NH-biotin)](PF$_6$)·2H$_2$O: C, 45.85; H, 4.01; N, 10.24. Found: C, 45.99; H, 3.89; N, 10.22. IR (KBr): ν(cm^{-1}) 3452 (m, NH), 2028 (s, C≡O), 1920 (s, C≡O), 1660 (s, C═O), 840 (s, PF_6^-). Positive-ion ESI-MS: m/z 1050 [Re(dppn)(CO)$_3$(py-CH$_2$NHCOC$_5$H$_{10}$NH-biotin)]$^+$, 603 [Re(dppn)(CO)$_3$]$^+$.

Physical Measurements, Instrumentation, and Titration Details. ^{1}H NMR spectra were recorded on a Varian Mercury 300 MHz NMR spectrometer at 298 K. Positive-ion ESI mass spectra were recorded on a Perkin-Elmer Sciex API 365 mass spectrometer. IR spectra were recorded on a Perkin-Elmer 1600 series FT-IR spectrophotometer. Elemental analysis was carried out on an Elementar Analyzensysteme GmbH Vario EL elemental analyzer or a Carlo Erba 1106 elemental analyzer at the Institute of Chemistry, Chinese Academy of Sciences. Electronic absorption spectra were recorded on a Hewlett-Packard 8453 diode array spectrophotometer. Steady-state excitation and emission spectra were recorded on a Spex Fluorolog-2 Model F 111 or a Fluoromax-3 fluorescence spectrophotometer. Unless specified otherwise, all solutions for photophysical studies were degassed with no fewer than four successive freeze−pump−thaw cycles and stored in a 10 cm^3 round-bottomed flask equipped with a 1 cm sidearm fluorescence cuvette and sealed from the atmosphere by a Rotaflo HP6/6 quick-release Teflon stopper. Luminescence quantum yields were measured by the optically dilute method[18] using an aerated aqueous solution of [Ru(bpy)$_3$]Cl$_2$ (Φ = 0.028) as the standard solution.[19] The excitation source for emission

(17) Fredericks, S. M.; Luong, J. C.; Wrighton, M. S. *J. Am. Chem. Soc.* **1979**, *101*, 7415.
(18) Demas, J. N.; Crosby, G. A. *J. Phys. Chem.* **1971**, *75*, 991.
(19) Nakamaru, K. *Bull. Chem. Soc. Jpn.* **1982**, *55*, 2697.

32lifetime measurements was the 355 nm output (third harmonic) of a Quanta-Ray Q-switched GCR-150-10 pulsed Nd:YAG laser. Luminescence decay signals from a Hamamatsu R928 photomultiplier tube were converted to potential changes by a 50 Ω load resistor and then recorded on a Tektronix Model TDS 620A (500 MHz, 2 GS/s) digital oscilloscope and analyzed using a program for exponential fits on an IBM-compatible computer. The electrochemical measurements were performed on a CH Instruments Electrochemical Workstation CHI750A. The electrochemical experiments were carried out at room temperature using a two-compartment glass cell with a working volume of 500 μL. A platinum-gauze counter electrode was accommodated in the working electrode compartment. The working and reference electrodes were a glassy-carbon electrode and an $Ag/AgNO_3$ (0.1 mol dm^{-3} $^nBu_4NPF_6$ in CH_3CN) electrode, respectively. The reference electrode compartment was connected to the working electrode compartment via a Luggin capillary. Solutions for electrochemical measurements were degassed with prepurified argon gas. All potentials were referred to SCE.

For the determination of binding constants for complexes **1** and **2** with double-stranded calf thymus DNA in the absorption titration experiments, the following fitting model was adopted:[20,21]

$$\frac{(\epsilon_a - \epsilon_f)}{(\epsilon_b - \epsilon_f)} = \frac{\left(b - \sqrt{b^2 - \frac{2K^2C_t[\mathrm{DNA}]}{s}}\right)}{2KC_t} \quad (1)$$

$$b = 1 + KC_t + \frac{K[\mathrm{DNA}]}{2s} \quad (2)$$

where ϵ_a is the extinction coefficient observed for the absorption band at a given DNA concentration ([DNA]), ϵ_b and ϵ_f are the extinction coefficients of bound and free forms of the complex, K is the intrinsic binding constant of the complex with the DNA, C_t is the total concentration of the rhenium(I) complex, and s is the binding site size in base pairs. A similar fitting procedure was performed for the emission titration experiments using emission intensity data instead of extinction coefficients in eq 1.

In the cases of complexes **3** and **4**, no satisfactory fits were obtained from the absorption titration data, perhaps due to cooperativity effects. The intrinsic binding constants K for complexes **3** and **4** with double-stranded calf thymus DNA were determined using another equation:[22]

$$\frac{D}{\Delta\epsilon_{ap}} = \frac{D}{\Delta\epsilon} + \frac{1}{\Delta\epsilon K} \quad (3)$$

where D is the concentration of DNA in base pairs, $\Delta\epsilon_{ap} = \epsilon_a - \epsilon_f$, and $\Delta\epsilon = \epsilon_b - \epsilon_f$, where ϵ_a, ϵ_f, and ϵ_b are the extinction coefficients of apparent, free, and bound forms of the rhenium(I) complex, respectively. The ϵ_a value is obtained by calculating A_{obs}/[Re]. A plot of $D/\Delta\epsilon_{ap}$ vs D will give a straight line with a slope of $1/\Delta\epsilon$ and a y intercept of $1/(\Delta\epsilon K)$. Thus, the intrinsic binding constant is given by the ratio of the slope to the y intercept.

The avidin-binding properties of the complexes were studied by luminescence titration experiments in degassed 50 mM potassium phosphate buffer at pH 7.2 at 298 K. For solubility reasons, the metal complexes were dissolved in DMSO to prepare the stock solutions. First dissociation constants K_d of the avidin−rhenium adducts were determined using the equation[23]

$$K_d = \frac{(n[\mathrm{P}]_0 - \alpha[\mathrm{L}]_0)^2}{(1-\alpha^2)([\mathrm{L}]_0 - n[\mathrm{P}]_0)} \quad (4)$$

where n is the binding stoichiometry, which is equal to 4 for the complexes in this work, $[P]_0$ and $[L]_0$ are the initial concentrations of the protein and the stock metal complex concentration, respectively, and $\alpha = V^*_c/V_0$, where V^*_c and V_0 are the volume of the metal complex solution added to attain the maximum observed changes in the spectroscopic signal and the initial volume of the protein solution, respectively.

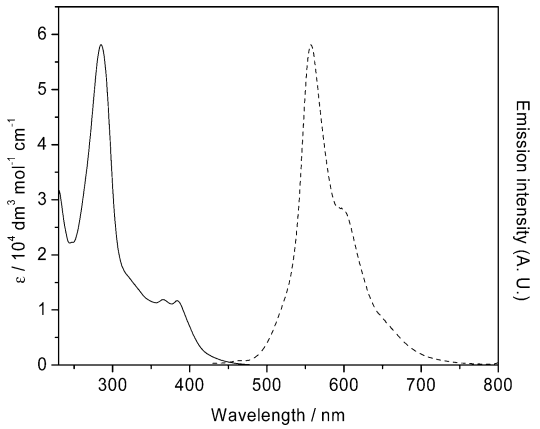

Figure 1. Electronic absorption (—) and emission (- - -) spectra of complex **1** in CH_2Cl_2 at 298 K.

Table 1. Electronic Absorption Spectral Data for Complexes 1−4 at 298 K

complex	medium	λ_{abs}/nm (ϵ/dm^3 mol^{-1} cm^{-1})
1	CH_2Cl_2	286 (57 980), 332 sh (14 225), 365 (12 100), 384 (11 920)
	CH_3CN	278 (64 930), 363 (12 845), 382 (12 835)
2	CH_2Cl_2	285 (62 535), 316 sh (18 250), 365 (12 930), 384 (12 690)
	CH_3CN	279 (55 650), 363 (11 100), 382 (11 115)
3	CH_2Cl_2	266 (34 620), 282 sh (27 385), 334 (46 355), 383 sh (8585), 403 (9185), 425 (8630)
	CH_3CN	241 (35 730), 262 (36 800), 280 sh (28 215), 323 (58 390), 376 sh (8515), 397 (9600), 419 (10 055)
4	CH_2Cl_2	265 (41 805), 284 sh (30 910), 333 (57 575), 380 sh (10 210), 402 (10 895), 425 (10 365)
	CH_3CN	246 (34 065), 262 (38 795), 279 sh (30 205), 324 (62 780), 376 sh (8790), 398 (10 045), 419 (10 660)

Results and Discussion

Synthesis. The rhenium(I) diimine biotin complexes **1**−**4** are prepared in moderate yields from the reactions of $[Re(N\text{-}N)(CO)_3(CH_3CN)](CF_3SO_3)$[17] (N-N = dppz, dppn) and the ligands py-CH_2NH-biotin[14] and py-$CH_2NHCOC_5H_{10}$NH-biotin in THF/MeOH, followed by metathesis with KPF_6 and purification by column chromatography. All the new complexes have been characterized by ^{1}H NMR, positive-ion ESI-MS, and IR and gave satisfactory elemental analysis. The complexes are soluble in common organic solvents such as alcohols, acetone, and chlorinated solvents but are only slightly soluble in water.

Electronic Absorption and Emission Properties. The electronic absorption spectral data of complexes **1**−**4** are summarized in Table 1. The electronic absorp-

(20) Carter, M. T.; Rodriguez, M.; Bard, A. J. *J. Am. Chem. Soc.* **1989**, *111*, 8901.
(21) Smith, S. R.; Neyhart, G. A.; Kalsbeck, W. A.; Thorp, H. H. *New J. Chem.* **1994**, *18*, 397.
(22) Wolfe, A.; Shimer, G. H., Jr.; Meehan, T. *Biochemistry* **1987**, *26*, 6392.
(23) Wang, Z.-X.; Kumar, N. R.; Srivastava, D. K. *Anal. Biochem.* **1992**, *206*, 376.

Table 2. Photophysical Data of Complexes 1−4

complex	medium (*T*/K)	λ_{em}/nm	τ_o/μs	Φ	I (τ/μs)[a,b]	I (τ/μs)[a,c]	I (τ/μs)[a,d]
1	CH_2Cl_2 (298)	558, 601 sh	4.90	0.0049	1.00 (0.39)	39.87 (0.91)	0.85 (0.39)
	CH_3CN (298)	556, 599 sh	7.12	0.0016			
	glass (77)[e]	547 (max), 562 sh, 592, 614 sh, 645 sh	12887				
2	CH_2Cl_2 (298)	556, 607 sh	4.50	0.0049	1.00 (0.28)	1.92 (0.50)	0.89 (0.26)
	CH_3CN (298)	554, 597 sh	8.01	0.0031			
	glass (77)[e]	544 (max), 559 sh, 590, 612 sh, 638 sh	12405				
3	CH_2Cl_2 (298)	587	17.88	0.20	1.00 (0.26)	3.65 (0.40)	1.28 (0.27)
	CH_3CN (298)	595	31.47	0.13			
	glass (77)[e]	517, 556 (max), 603 sh	5.77				
4	CH_2Cl_2 (298)	588	22.15	0.23	1.00 (0.22)	2.39 (0.29)	1.09 (0.20)
	CH_3CN (298)	595	33.09	0.095			
	glass (77)[e]	524, 558 (max), 607 sh	6.72				

[a] Relative emission intensities in degassed 50 mM potassium phosphate buffer at pH 7.2. [b] Conditions: [Re] = 15.2 μM, [avidin] = 0 μM, [unmodified biotin] = 0 μM. [c] Conditions: [Re] = 15.2 μM, [avidin] = 3.8 μM, [unmodified biotin] = 0 μM. [d] Conditions: [Re] = 15.2 μM, [avidin] = 3.8 μM, [unmodified biotin] = 380.0 μM. [e] EtOH/MeOH (4/1 v/v).

tion spectrum of complex **1** in CH_2Cl_2 at 298 K is shown in Figure 1. The absorption characteristics of the complexes are similar to those of their structural analogues $[Re(N\text{-}N)(CO)_3(py)]^+$ (N-N = dppz, dppn).[9] This is reasonable, because the amide and thioether of the biotin moiety and the amide of the linker are not expected to exhibit absorption in the visible region. The absorption bands of the complexes at ca. 241−334 nm (ϵ on the order of 10^4 dm^3 mol^{-1} cm^{-1}) are assigned to ^{1}IL (N-N and pyridine) transitions. The complexes display moderately intense absorption shoulders and bands in the visible region (ca. 363−425 nm). With reference to previous spectroscopic work on related rhenium(I) diimine complexes,[7−9,14,17,24−34] these absorption features are assigned to ^{1}MLCT ($d\pi(Re) \rightarrow \pi^*(N\text{-}N)$) transitions. It is likely that these transitions have considerable intraligand ^{1}IL character, given that the free dppz and dppn ligands also absorb in a similar region.[7−9] The lowest-energy MLCT/IL absorption bands of the dppz complexes **1** and **2** (ca. 364 and 383 nm) occur at a higher energy than those of the dppn complexes **3** and **4** (ca. 400 and 422 nm). This is in accordance with the more extended π-conjugation of the ligand dppn, which stabilizes the empty π^* orbitals of the dppn ligand and thus lowers the ^{1}MLCT and ^{1}IL transition energy of complexes **3** and **4**.

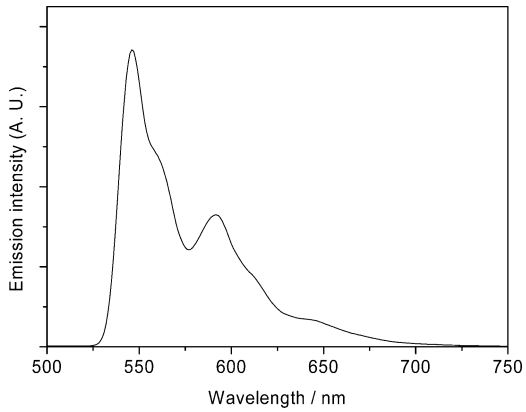

Figure 2. Emission spectrum of complex **1** in EtOH/MeOH (4/1 v/v) at 77 K.

Excitation of the complexes in solutions at room temperature and in low-temperature alcohol glass at λ_{ex} >350 nm gives rise to intense and long-lived greenish yellow to orange luminescence. All the emission decays are single exponential at 298 and 77 K. The photophysical data of complexes **1**−**4** are listed in Table 2. The emission spectrum of complex **1** in CH_2Cl_2 at room temperature is shown in Figure 1 as an example. The dppz complexes **1** and **2** showed an emission maximum at ca. 556 nm and a shoulder at ca. 600 nm in fluid solutions at 298 K. These structural features, as well as the extraordinarily low emission quantum yields (on the order of 10^{-3}) and long emission lifetimes, suggest that the excited state bears a high degree of ^{3}IL character associated with the dppz ligand. Similar observations have been reported in other rhenium(I) dppz complexes.[7−9] In low-temperature glass, rich vibronic structures are apparent in the emission spectra. The emission spectrum of complex **1** in a low-temperature alcohol glass is shown in Figure 2. Progressional spacings of ca. 1300−1800 cm^{-1} that are typical of aromatic C⋯C

(24) (a) Wrighton, M. S.; Morse, D. L. *J. Am. Chem. Soc.* **1974**, *96*, 998. (b) Giordano, P. J.; Wrighton, M. S. *J. Am. Chem. Soc.* **1979**, *101*, 2888.

(25) (a) Shaver, R. J.; Rillema, D. P. *Inorg. Chem.* **1992**, *31*, 4101. (b) Wallace, L.; Rillema, D. P. *Inorg. Chem.* **1993**, *32*, 3836. (c) Wallace, L.; Jackman, D. C.; Rillema, D. P.; Merkert, J. W. *Inorg. Chem.* **1995**, *34*, 5210.

(26) (a) Westmoreland, T. D.; Le Bozec, H.; Murray, R. W.; Meyer, T. J. *J. Am. Chem. Soc.* **1983**, *105*, 5952. (b) Worl, L. A.; Duesing, R.; Chen, P.; Ciana, L. D.; Meyer, T. J. *J. Chem. Soc., Dalton Trans.* **1991**, 849. (c) Claude, P. J.; Omberg, K. M.; Williams, D. S.; Meyer, T. J. *J. Phys. Chem. A* **2002**, *106*, 7795.

(27) (a) Thornton, N. B.; Schanze, K. S. *Inorg. Chem.* **1993**, *32*, 4994. (b) Thornton, N. B.; Schanze, K. S. *New J. Chem.* **1996**, *20*, 791. (c) Lucia, L. A.; Abboud, K.; Schanze, K. S. *Inorg. Chem.* **1997**, *36*, 6224.

(28) (a) Lees, A. J. *Chem. Rev.* **1987**, *87*, 711. (b) Sun, S.-S.; Lees, A. J. *Organometallics* **2002**, *21*, 39. (c) Sun, S.-S.; Lees, A. J.; Zavalij, P. Y. *Inorg. Chem.* **2003**, *42*, 3445.

(29) Juris, A.; Campagna, S.; Bidd, I.; Lehn J.-M.; Ziessel, R. *Inorg. Chem.* **1988**, *27*, 4007.

(30) (a) Moya, S. A.; Guerrero, J.; Pastene, R.; Schmidt, R.; Sariego, R.; Sartori, R.; Sanz-Aparicio, J.; Fonseca, I.; Martínez-Ripoll, M. *Inorg. Chem.* **1994**, *33*, 2341. (b) Guerrero, J.; Piro, O. E.; Wolcan, E.; Feliz, M. R.; Ferraudi, G.; Moya, S. A. *Organometallics* **2001**, *20*, 2842.

(31) (a) Sacksteder, L.; Zipp, A. P.; Brown, E. A.; Streich, J.; Demas, J. N.; DeGraff, B. A. *Inorg. Chem.* **1990**, *29*, 4335. (b) Zipp, A. P.; Sacksteder, L.; Streich, J.; Cook, A.; Demas, J. N.; DeGraff, B. A. *Inorg. Chem.* **1993**, *32*, 5629. (c) Sacksteder, L.; Lee, M.; Demas, J. N.; DeGraff, B. A. *J. Am. Chem. Soc.* **1993**, *115*, 8230.

(32) (a) Sullivan, B. P. *J. Phys. Chem.* **1989**, *93*, 24. (b) Hino, J. K.; Ciana, L. D.; Dressick, W. J.; Sullivan, B. P. *Inorg. Chem.* **1992**, *31*, 1072. (c) Schutte, E.; Helms, J. B.; Woessner, S. M.; Bowen, J.; Sullivan, B. P. *Inorg. Chem.* **1998**, *37*, 2618.

(33) (a) Yoblinski, B. J.; Stathis, M.; Guarr, T. F. *Inorg. Chem.* **1992**, *31*, 5. (b) Lin, R.; Fu, Y.; Brock, C. P.; Guarr, T. F. *Inorg. Chem.* **1992**, *31*, 4346.

(34) (a) Lo, K. K. W.; Ng, D. C. M.; Hui, W. K.; Cheung, K. K. *Dalton* **2001**, 2634. (b) Lo, K. K. W.; Hui, W. K.; Ng, D. C. M.; Cheung, K. K. *Inorg. Chem.* **2002**, *41*, 40. (c) Lo, K. K. W.; Tsang, K. H. K.; Hui, W. K.; Zhu, N. *Chem. Commun.* **2003**, 2704.

Table 3. Electrochemical Data for Complexes 1−4 at 298 K[a]

complex	oxidn, $E_{p,a}$/V	redn, $E_{1/2}$ or $E_{p,c}$/V
1	+1.80[b]	−0.92, −1.38,[b] −1.45,[b] −1.55,[c] −1.69[c]
2	+1.77[b]	−0.92, −1.38,[b] −1.48,[b] −1.55, −1.72
3	+1.80[b]	−0.71, −1.14,[c] −1.41,[c] −1.56,[c] −1.72[c]
4	+1.81[b]	−0.72, −1.20,[c] −1.42,[c] −1.59, −1.72[c]

[a] Conditions: in CH_3CN (0.1 mol dm^{-3} $^nBu_4NPF_6$), glassy-carbon electrode, sweep rate 100 mV s^{-1}, all potentials vs SCE. [b] Irreversible waves. [c] Quasi-reversible couples.

and C⋯N stretches are observed. The emission lifetimes are very long (ca. 12 ms), and it is likely that the emission originates from an ^{3}IL (dppz) excited state.[7−9]

The solution emission of the dppn complexes **3** and **4** appears as a structureless broad band with a peak maximum at ca. 587−595 nm. The emission lifetimes (ca. 18−33 μs) are longer than those of their dppz counterparts, but the emission quantum yields (ca. 0.1−0.2) are comparable to common rhenium(I) polypyridine ^{3}MLCT emitters.[15,24b,25−29,30b,31−34] We tentatively assign the emission to an ^{3}IL (dppn) excited state. However, it is likely that ^{3}MLCT (dπ(Re) → π^*(dppn)) character is also present in the emissive state of these complexes. Vibronically structured emission spectra are observed for complexes **3** and **4** in low-temperature glasses. The emission is assigned to an ^{3}IL (dppn) excited state. It is noteworthy that (i) the emission maxima of complexes **3** and **4** (ca. 556−558 nm) occur at slightly lower energy than those of the dppz complexes (ca. 544−547 nm) and (ii) the emission lifetimes are much shorter (ca. 6 μs) than those of complexes **1** and **2**. These observations suggest that the excited states of complexes **3** and **4** also involve substantial ^{3}MLCT character. The similar photophysical data of complexes **1** and **2**, and of complexes **3** and **4**, clearly indicates that the presence of spacer arms between the pyridine and the biotin moiety does not have a significant effect on the emission properties of the complexes.

Electrochemical Properties. The electrochemical properties of complexes **1**−**4** have been studied by cyclic voltammetry. The electrochemical data are listed in Table 3. With reference to previous electrochemical studies of rhenium(I) diimine complexes,[25a,b,26a,c,27c,28b,30b,31,32b,33,34c] the irreversible waves at ca. +1.80 vs SCE for all four complexes are assigned to the rhenium(II/I) oxidation couple. The first reversible reduction couples at ca. −0.92 V for the dppz complexes and ca. −0.71 V for the dppn complexes are assigned to reduction of the diimine ligands. The less negative potential for the dppn complexes as compared to that of the dppz complexes is due to the more extended π-conjugation of the dppn ligand. The potentials of the oxidation waves and first reduction couples of complexes **1**−**4** are very similar to those of their biotin-free analogues $[Re(dppz)(CO)_3(py)]^+$ (ca. +1.79 and −0.94 V, respectively) and $[Re(dppn)(CO)_3(py)]^+$ (ca. +1.78 and −0.83 V, respectively),[35] suggesting the lack of involvement of the biotin groups on the electrochemical behavior of the complexes. Additionally, complexes **1**−**4** exhibit quasi-reversible and irreversible waves at more negative potentials, which are tentatively assigned to the reduction of the diimine ligands, except for those at ca. −1.45 V, which could be assigned to the rhenium(I/0) couple.[33b]

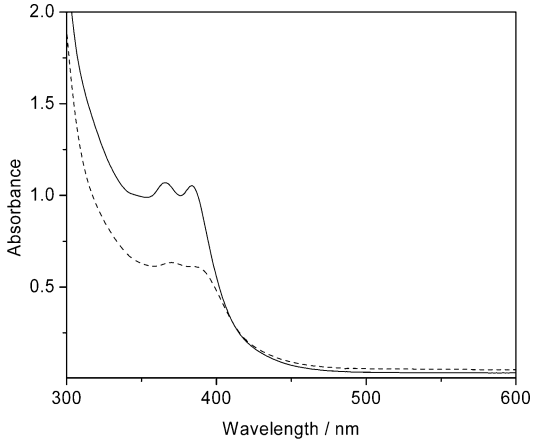

Figure 3. Electronic spectral traces of complex **1** (80 μM) in 20 mM Tris-Cl at pH 7.2/methanol (7/3 v/v) in the absence (—) and presence (- - -) of double-stranded calf thymus DNA (673 μM).

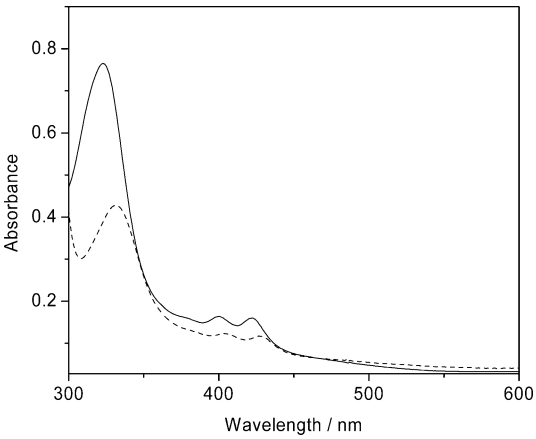

Figure 4. Electronic spectral traces of complex **3** (20 μM) in 20 mM Tris-Cl at pH 7.2/methanol (7/3 v/v) in the absence (—) and presence (- - -) of double-stranded calf thymus DNA (192 μM).

DNA Binding. The DNA-binding properties of complexes **1**−**4** have been studied by absorption and emission titration experiments. For solubility reasons, the experiments were carried out in a mixture of 20 mM Tris-Cl buffer at pH 7.2 and methanol (7/3 v/v). Upon addition of double-stranded calf thymus DNA, the low-energy absorption bands of the dppz complexes **1** and **2** at 366 and 384 nm exhibit pronounced hypochromism and a small bathochromic shift. Similar changes are also observed for the absorption bands of the dppn complexes **3** and **4** at 323, 400, and 422 nm. To illustrate this, the electronic absorption spectral traces for complexes **1** and **3** in the absence and presence of double-stranded calf thymus DNA are shown in Figures 3 and 4, respectively. No similar hypochromism and bathochromic shifts are observed when single-stranded calf thymus DNA is used. These findings, together with the changes in the absorption spectra, suggest that the complexes bind to double-stranded calf thymus DNA by intercalation.[36] Similar observations have been reported for many transition-metal complexes containing dppz and dppn ligands.[2−9]

(35) Yam, V. W. W.; Lo, K. K. W. Unpublished results.
(36) Bloomfield, V. A.; Crothers, D. M.; Tinoco, I. J. *Physical Chemistry of Nucleic Acid*; Harper and Row: New York, 1974.

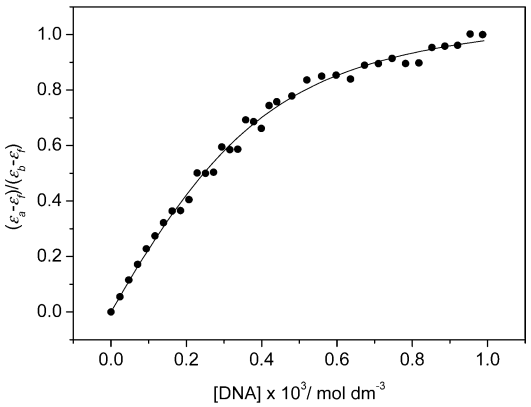

Figure 5. Plot of $(\epsilon_a - \epsilon_f)/(\epsilon_b - \epsilon_f)$ vs [DNA] for the binding of complex **1** (80 μM) to double-stranded calf thymus DNA. The experimental data obtained at $\lambda_{abs} = 366$ nm are fitted using eqs 1 and 2.

Table 4. DNA-Binding Parameters for Complexes 1−4 to Double-Stranded Calf Thymus DNA in 20 mM Tris-Cl at pH 7.2/Methanol (7/3 v/v) at 298 K

	intrinsic binding constant, K/M^{-1} (binding site size, s)	
complex	UV−vis	emission
1	1.0×10^4 (0.76)	8.8×10^3 (0.69)
2	1.1×10^4 (0.82)	9.2×10^3 (0.70)
3	3.5×10^4 (−)[a]	3.8×10^4 (0.73)
4	1.6×10^4 (−)[a]	1.7×10^4 (0.65)

[a] The binding site size cannot be determined from eq 3.

The intrinsic binding constants K for complexes **1** and **2** with double-stranded calf thymus DNA are calculated using eqs 1 and 2. The decay of the absorbance of complexes **1** and **2** at 366 nm is monitored upon addition of double-stranded DNA. A plot of $(\epsilon_a - \epsilon_f)/(\epsilon_b - \epsilon_f)$ vs [DNA] for complex **1** is shown in Figure 5. Fitting of the experimental data to eqs 1 and 2 gives intrinsic binding constants of 1.0×10^4 and 1.1×10^4 M^{-1} for the binding of complexes **1** and **2** to double-stranded calf thymus DNA, respectively (Table 4). The binding site size is determined to be ca. 0.8 for both complexes (Table 4).

Unfortunately, similar to the case for $[Re(dppn)(CO)_3(py)]^+$,[9b] no satisfactory fits are obtained from the absorption data of complexes **3** and **4**, perhaps due to cooperativity effects. The intrinsic binding constants for these two complexes with double-stranded calf thymus DNA are calculated using eq 3. The decay of the absorbance of the dppn complexes **3** and **4** at 323 nm is monitored upon addition of double-stranded DNA. A plot of $D/\Delta\epsilon_{ap}$ vs D for the binding of complex **3** and the theoretical fit are shown in Figure 6. Intrinsic binding constants of complexes **3** and **4** to double-stranded calf thymus DNA are determined to be 3.5×10^4 and 1.6×10^4 M^{-1}, respectively (Table 4).

In addition, the DNA-binding properties of the complexes have been studied by emission titration experiments. In 20 mM Tris-Cl at pH 7.2/methanol (7/3 v/v), the emission of complexes **1**−**4** is enhanced in the presence of double-stranded calf thymus DNA. The emission spectral traces for complex **1** with double-stranded calf thymus DNA are displayed in Figure 7 as an example. Similar emission enhancements have been commonly observed for other luminescent dppz complexes, and they are due to the intercalation of the

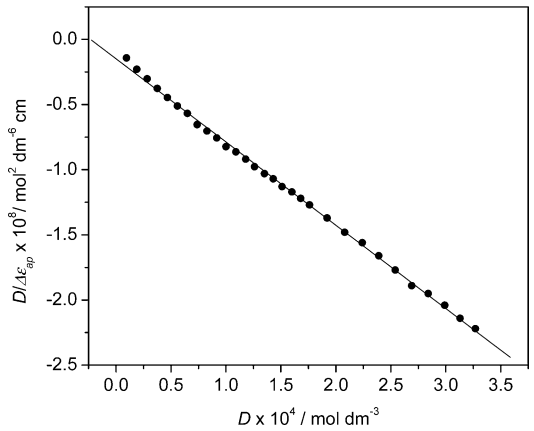

Figure 6. Plot of $D/\Delta\epsilon_{ap}$ vs D for the binding of complex **3** (20 μM) to double-stranded calf thymus DNA. The experimental data obtained at $\lambda_{abs} = 323$ nm are fitted using eq 3.

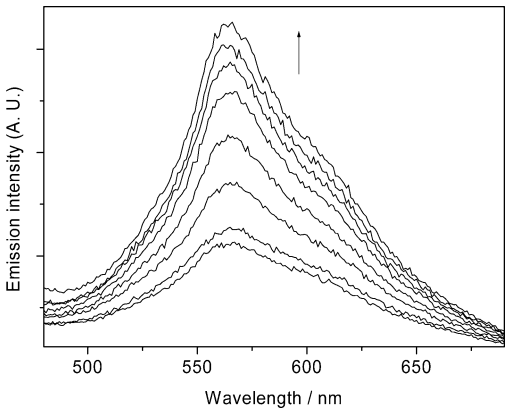

Figure 7. Emission spectral traces of complex **1** (80 μM) in 20 mM Tris-Cl at pH 7.2/methanol (7/3 v/v) at 298 K in the presence of 0, 24, 119, 239, 358, 477, 620, and 1145 μM double-stranded calf thymus DNA.

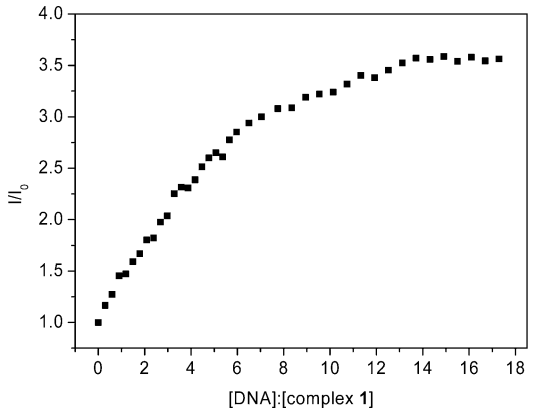

Figure 8. Emission titration curve for complex **1** with double-stranded calf thymus DNA. The emission intensity of complex **1** is monitored at 565 nm.

complexes to double-stranded DNA. The emission titration curves for complexes **1** and **3** with double-stranded calf thymus DNA are shown in Figures 8 and 9, respectively. The emission intensities of the dppz complexes **1** and **2** are increased by ca. 3.5-fold. For the dppn complexes **3** and **4**, the emission intensities also increase and become saturated with an overall gain of ca. 2.2. Data from the emission titrations are fitted to eqs 1 and 2 to determine the intrinsic binding constants.

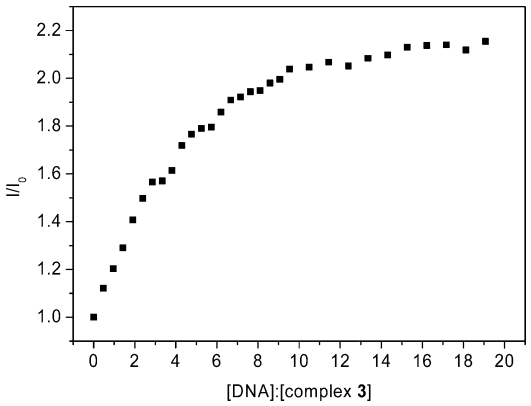

Figure 9. Emission titration curve for complex **3** with double-stranded calf thymus DNA. The emission intensity of complex **3** is monitored at 612 nm.

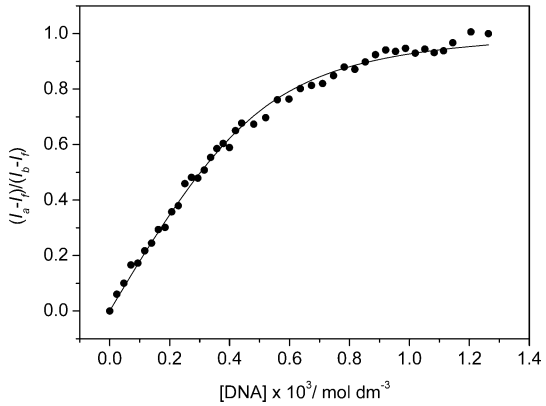

Figure 10. Plot of $(I_a - I_f)/(I_b - I_f)$ vs [DNA] for the binding of complex **1** (80 μM) to double-stranded calf thymus DNA. The emission intensity is monitored at 565 nm.

A plot of $(I_a - I_f)/(I_b - I_f)$ vs [DNA] for complex **1** is shown in Figure 10. The binding parameters (Table 4) agree very well with those obtained using the absorption titration data. In general, the intrinsic binding constants of complexes **1**−**4** are 1−2 orders of magnitude smaller than those of structural analogues such as $[Re(dppz)(CO)_3(4\text{-Mepy})]^+$ (4-Mepy = 4-methylpyridine; 4×10^6 M^{-1})[7] and $[\{Re(dppz)(CO)_3\}_2(BL)]^{2+}$ (BL = 1,2-bis(4-pyridyl)ethane, 1,3-bis(4-pyridyl)propane; 7×10^5 M^{-1}).[8] A possible reason is that different buffer systems are used in the experiments. In the current work, due to solubility reasons, the titration experiments are performed in a mixture of 20 mM Tris-Cl at pH 7.2 and methanol (7/3 v/v), and such a high methanol content appears to lower the binding constants. However, it is noteworthy that the binding constants of complexes **1**−**4** with double-stranded calf thymus DNA are smaller than those of the biotin-free analogues $[Re(dppz)(CO)_3(py)]^+$ (4.2×10^4 M^{-1}) and $[Re(dppn)(CO)_3(py)]^+$ (6.4×10^4 M^{-1}) in the same buffer system.[9] These observations are probably due to the steric hindrance between the biotin moieties of the complexes and the double-stranded DNA molecules. The binding constants of the dppz complexes **1** and **2** are very similar, indicating that the presence of a 6-aminocaproic acid linker does not substantially enhance the binding interactions. However, it is interesting to note that the binding constant of complex **3** doubles that of complex **4** (Table 4). On the basis of the assumption that the linker does not effectively alleviate the steric hindrance between the complex and DNA molecules, a possible reason for the difference is that, in complex **4**, the hydrophobic rhenium−dppn moiety interacts strongly with the 6-aminocaproic acid spacer arm in a highly polar aqueous buffer/methanol environment. This hydrophobic interaction is likely to reduce the efficiency of the intercalation of the dppn moiety into the base pairs of the double-stranded DNA molecules, which thus leads to a lower binding affinity.

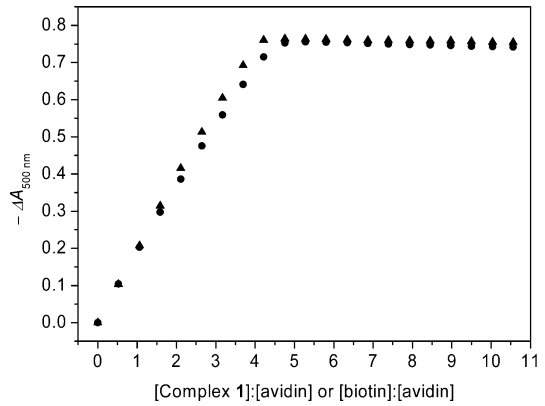

Figure 11. Plots of $-\Delta A_{500\ nm}$ vs [complex **1**]:[avidin] or [biotin]:[avidin] for the binding of complex **1** (●) and unmodified biotin (▲) to avidin in the HABA assays. The concentrations of HABA and avidin were 0.3 mM and 7.6 μM, respectively.

Avidin Binding. The avidin-binding properties of complexes **1**−**4** are investigated using the standard HABA assay[11,12] and emission titration experiments.[13] Binding of HABA to avidin is associated with an increase in the absorbance at 500 nm, owing to the formation of the quinone tautomer of HABA at the biotin-binding site of the protein. Additions of complexes **1**−**4** into a mixture of HABA (0.3 mM) and avidin (7.6 μM) result in a decrease of the absorbance at 500 nm, indicating that the bound HABA molecules are replaced by the rhenium(I) polypyridine biotin complexes. The HABA assay results indicate that complexes **1**−**4** bind to the avidin molecule with the same stoichiometry as unmodified biotin (biotin:avidin = 4:1). A plot of $-\Delta A_{500\ nm}$ vs [complex **1**]:[avidin] or [biotin]:[avidin] is shown in Figure 11 as an example.

Luminescence titrations using the complexes as the titrants show that emission intensities of complexes **1**−**4** are all enhanced in the presence of avidin. At [rhenium]:[avidin] = 4:1, the emission intensity of complex **1** at 570 nm is ca. 40 times higher than that in the absence of avidin (Figure 12). For complexes **2**−**4**, the enhancement factors vary from ca. 1.9 to 3.7 (Table 2). The emission titration curves for complex **1** are shown in Figure 13. The emission lifetimes of all the complexes also increase by ca. 1.3−2.3-fold, and all the decays remain single exponential. We attribute the enhancement in emission intensities and the lifetime elongation to the binding of biotin moieties of the complexes into the biotin-binding sites of avidin, because no similar changes are observed when the avidin solution is presaturated with unmodified biotin (Table 2 and Figure 13). Similar observations have been reported for the rhenium(I) polypyridine biotin complexes that we reported recently.[14]

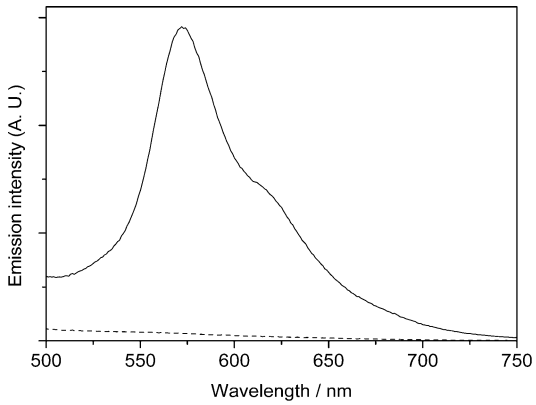

Figure 12. Emission spectra of complex **1** (15.2 μM) in the absence (- - -) and presence (—) of avidin (3.8 μM) in degassed 50 mM potassium phosphate buffer at pH 7.2/DMSO (97/3 v/v) at 298 K.

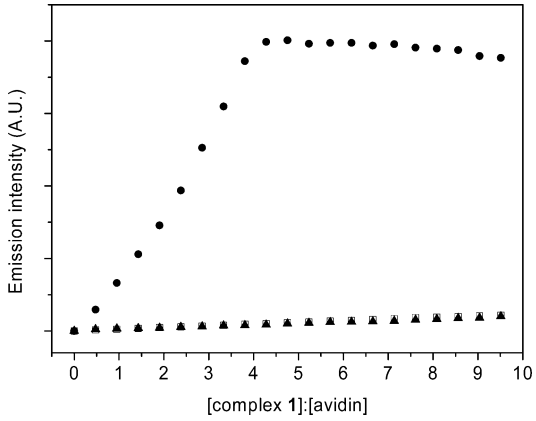

Figure 13. Luminescence titration curves for the titration of (i) 3.8 μM avidin (●), (ii) 3.8 μM avidin and 380.0 μM unmodified biotin (▲), and (iii) a blank phosphate buffer solution (□) with complex **1**.

It is important to mention that traditional fluorescent biotin conjugates exhibit significant emission quenching due to effective resonance-energy transfer (RET) when they bind to avidin. Fluorescence can only be observed when long spacer arms are present between the biotin moiety and the fluorophore, to separate the organic dyes upon binding to avidin. In the current study, the absence of emission quenching is a result of the insignificant overlap between the absorption and emission bands of the complexes, which renders RET quenching unfavorable. The emission enhancement is in agreement with the observations that when luminescent transition metal complexes are conjugated to protein molecules, the emission is enhanced. We believe that the emission intensity enhancement of complexes **1**—**4** is due to an increase in the hydrophobicity of the local surroundings of the complex after the binding of the biotin moiety to avidin. The mechanism may be similar to that of DNA binding—intercalation of the complexes to the DNA duplex could isolate the complex from the polar aqueous surroundings and result in an increase of emission intensity and lifetimes. Another possible reason is the increased rigidity of the environment of the complexes that leads to a lower nonradiative decay efficiency.

Using eq 4, first dissociation constants for the avidin—rhenium adducts are determined to be ca. 1.1×10^{-9}, 5.4×10^{-9}, 1.9×10^{-9}, and 4.4×10^{-9} M for complexes **1**—**4**, respectively. The constants are all of the same order of magnitude. It is interesting to note that the 6-aminocaproic acid spacer arms of complexes **2** and **4** do not significantly enhance their binding to avidin compared to complexes **1** and **3**. Similar to the reasons given in the previous section, we cannot exclude the possibility that the hydrophobic interaction between the linkers and the extended planar diimine ligands suppresses the binding of complexes **2** and **4** to avidin. Finally, we investigate the possibility of using complexes **1**—**4** as a cross-linker for double-stranded DNA and avidin. Unfortunately, precipitation of the reaction mixtures occurs, and it is likely that the hydrophobic nature of the complexes excludes their possible roles as a biological cross-linker due to solubility reasons.

Conclusion. A series of rhenium(I) complexes that contain an extended planar diimine ligand and a biotin moiety has been synthesized and characterized, and their photophysical and electrochemical properties have been investigated. The photophysical data indicate that the emission of the complexes originates from a triplet intraligand (^{3}IL) ($\pi \rightarrow \pi^*$) (diimine) excited state. However, the emissive states of the dppn complexes **3** and **4** are likely to contain substantial ^{3}MLCT (dπ(Re) $\rightarrow \pi^*$(dppn)) character. The interactions of complexes **1**—**4** with double-stranded calf thymus DNA have been studied by absorption and emission titrations. The complexes bind to the duplex by intercalation, with the planar diimine ligands stacked between the base pairs of the DNA. These luminescent rhenium(I) biotin complexes can also bind to the protein avidin, and the binding has been studied by HABA assays and emission titrations. Interestingly, all the complexes show emission enhancement and lifetime elongation upon binding to avidin. In particular, complex **1** displays a significant increase in emission intensity in the presence of avidin. From the results of this work, we anticipate that, with a judicious choice of ligands, new biosensors based on luminescent multifunctional complexes containing recognition elements for various biomolecules can be developed.

Acknowledgment. This work was fully supported by a Strategic Research Grant (Project No. 7001456) from the City University of Hong Kong. K.H.-K.T. acknowledges the receipt of a postgraduate studentship and a Research Tuition scholarship, both administered by the City University of Hong Kong. We are grateful to Professor Vivian W. W. Yam of The University of Hong Kong for access to the equipment for photophysical measurements.

OM049936X